Isı Bilimi ve Tekniği Dergisi, 39, 1, 17-30, 2019
J. of Thermal Science and Technology

ISSN 1300-3615

FORCED CONVECTION HEAT TRANSFER IN A POWER-LAW FLUID FLOW IN A CIRCULAR DUCT

Fethi KAMIŞLI
Department of Chemical Engineering, Firat University, 23119 Elazig, Turkey.
E-mail: fkamisli@firat.edu.tr. Fax: +90 424 241 5526, Tlf: +90 424 237 0000 ext:5515

(Geliş Tarihi: 14.05.2018, Kabul Tarihi: 16.01.2019)

Abstract: The dimensionless temperature, the entropy generation rate and Nusselt number for a power-law fluid flow in a pipe with constant wall heat flux have been determined as functions of the Brinkman number, power-law index, dimensionless temperature difference and group parameters. The one-dimensional approximate equations with viscous dissipation for the energy, the entropy and the Nusselt number for a power-law fluid flow have been determined by accounting for the order of magnitude of terms and asymptotic techniques. The one-dimensional approximate equations of the velocity, the temperature and the entropy generation rate have been analytically solved to determine the velocity, the temperature and the entropy distributions in a non-Newtonian fluid flow as functions of the effective process parameters. The derived equation with viscous dissipation term for Nusselt number depending on power-law index and Brinkman number covers all types of pseudo-plastic and dilatant fluid behaviors. It has found that the Brinkman number is quite effective on the temperature, the Nusselt number and the entropy generation number. The Nusselt number has exponentially decreased with increasing Brinkman number at values of power-law index.
Keywords: Brinkman number; entropy generation; viscous dissipation; power-law fluid flow.

DAİRESEL BİR BORUDA ÜST KANUNU AKIŞKANININ AKIŞINDA ZORLANMIŞ TAŞINIMLA ISI TRANSFERİ

Özet: Sabit duvar ısı akısına sahip bir boruda üst kanunu akışkan akışı için boyutsuz sıcaklık, entropi üretim hızı ve Nusselt sayısı, üst kanunu indeksi, Brinkman sayısı, boyutsuz sıcaklık farkı ve grup parametrelerinin fonksiyonu olarak belirlenmiştir. Üst kanunu akışkan akışında enerji, entropi ve Nusselt sayısı için sürtünme kaynaklı enerji üretim terimini içeren bir boyutlu yaklaşık eşitlikler; terimlerin büyüklük dereceleri ve asimptotik teknikler göz önünde bulundurularak çıkarılmıştır. Hız, sıcaklık ve entropi üretimi için bir boyutlu yaklaşık eşitlikler Newton kanununa uymayan akışkan akışını için hız, sıcaklık ve entropi dağılımlarını belirlemek için analitik olarak etkin parametrelerin fonksiyonu olarak çözümlenmiştir. Akış indeksi ve Brinkman sayına bağlı Nusselt sayısı için sürtünme kaynaklı enerji üretim terimli türetilmiş eşitlik, bütün pseudo plastik ve dilatant akışkan davranışlarını kapsamaktadır. Brinkman sayısının sıcaklık, entropi üretim sayısı ve Nusselt sayısı üzerinde oldukça etkin olduğu bulunmuştur. Üs kanununu indeksinin tüm değerlerinde Nusselt sayısı, Brinkman sayısının artmasıyla üstel olarak azalmıştır.
Anahtar Kelimeler: Entropy üretimi; zorlanmış taşınım; Brinkman sayısı; üst kanunu akışkanı akışı.

NOMENCLATURE

Be	Bejan number, Be = $(N_R+N_C)/(N_R+N_C+N_F)$
Br	Brinkman number ($Br = Pr \times Ec$)
C_i	Integration constants, i = 0-5
c_P	Specific heat capacity (J kg^{-1} °C^{-1})
D	Tube diameter (m)
Ec	Modified Eckert number, $Ec = v_{z\max}^{n+1} / \left(c_p \Delta T\, R^{(n-1)}\right)$ ve $\Delta T = q_0'' R / k$
Fr_i	Froude number in *i*-direction = v_0^2 / Lg_i
g_i	Gravity in i-direction (m/s^2)
G_i	Re/Fr_i
k	Thermal conductivity of fluid (W/m °C)
L	Length of tube (m)
Pe	Peclet number = $v_{z\max} \rho c_P R / k$
Pr	Prandtl number = $\eta_0 c_P / k$
q_0''	Constant heat flux at the tube wall (W/m^2)
R	Radius (m)
Re	Reynolds number = $\rho v_0 D / \eta_0$
γ	Modified power-law index = $1/n$
N_C	Entropy generation number due to conduction in axial direction
N_R	Entropy generation number due to conduction in radial direction
N_F	Entropy generation number due to fluid particles friction
N_S	Entropy generation number
S_G	Entropy generation rate (W/m^3 K)
T	Temperature (°C)
$T_r = T_0$	Reference temperature (°C)
v_i	Velocity in *i*-direction (m/s)

v_{zmax} Maximum velocity in axial direction (m/s)
z Axial distance (m)

Greek symbols
α Thermal diffusivity of the fluid (m^2/s)
η_0 Dynamic viscosity of the fluid (Ns/m^2)
ψ Dimensionless temperature $=(T-T_r)/(q_0''R/k)$
$\Omega=\Delta T/T_0$ Dimensionless temperature difference
ρ Density of the fluid (kg/m^3)
ϕ Irreversibility Ratio = Br/Ω
τ_{ij} Stress for ij sub-indices
ξ Dimensionless radius
ζ Dimensionless axial distance

INTRODUCTION

Many investigations on the flow of a Newtonian or a non-Newtonian fluid in a circular duct at low Reynolds number and the heat transfer with forced convection have long been performed due to its importance to a variety of situations. The heat convection processes in Newtonian and non-Newtonian fluids confined in a circular/non-circular tube has been intensively studied theoretically and analytically due to its importance for science and technology. The forced convection heat transfer occurs in increasing variety of modern instruments and systems such as micro-electro-mechanical system, laser-cooling system.

Thereby, to construct efficient equipment in terms of energy consumption efficiency is important since the useful energy will be conversed in this way, which requires thermodynamically efficient heat transfer processes. The thermodynamic irreversibility associated with fluid flow and heat transfer inside a circular or non-circular ducts at different boundary conditions is a subject of many researches (Bejan, 1979, 1982, Sahin, 1998, Narusawa, 2001).

Entropy generation in convective heat transfer in laminar flow of a Newtonian fluid confined in a circular duct with constant heat flux at wall was studied by Bejan (1979) to analyze entropy generation because of irreversibility due to heat transfer along the finite temperature gradient and irreversibility due to viscous effect. This work is extended by Bejan (1996) by adding calculation of the optimum Reynolds number as a function of Prandtl number and duty parameter. In another study, Bejan (1982) focus on a minimization of entropy generation due to irreversibility because of different reasons in applied engineering. Sahin (1998) extended Bejan's studies (1979, 1982) by performing a second law analysis of viscous fluids in a circular duct at constant wall temperature. In another study Sahin (1999) examined an effect of viscosity on the entropy generation rate for a heated circular duct.

Entropy generation in a Newtonian fluid flow and heat transfer in a rectangular duct were analytically and numerically analyzed by Narasuwa (2001). The second law optimization techniques were used by Nag and Kumar (1989) to analyze the convective heat transfer in a Newtonian fluid flow in a duct at constant heat flux.

Kamisli (2009) analyzed the flow of an incompressible Newtonian fluid confined in a planar geometry filled with a homogeneous and isotropic porous medium in terms of determining the unsteady state and steady state velocities, temperature and entropy generation rate as functions of the pressure drop, the Darcy number and Brinkman number. In another study, Kamisli (2008) performed analysis on fully developed laminar flow in a horizontal thin slit with the wall suction/injection in terms of entropy generation as functions of Prandtl number, Eckert number, cross-flow Reynolds number and the dimensionless temperature. Kamisli and Oztop (2008) performed a second law analysis of 2D laminar flow of two immiscible, incompressible viscous fluids in a channel in terms of determining entropy generation as functions of effective parameters such as the Prandtl number, the Eckert number and the viscous dissipation ratio.

Sahin (2014) recently studied on the entropy generation in a duct in an effort to develop a model to estimate entropy generation.

Unlike previous researchers Mahmud and Fraser (2006) examined thermodynamic irreversibility associated with the laminar flow of a non-Newtonian fluid confined in a circular at constant heat flux with a view to minimize entropy generation and thus to conserve useful energy. Souli and Aiboud-Souli (2009) studied on the entropy generation of power-law fluid flow on an inclined heated plate. Mukherjee et al. (2017) studied on forced convection in power-law and Bingham plastic fluids in different cross-sectional area of ducts. Thermal analysis of power-law fluid flow in a circular microchannel was performed by Sarabandi and Moghadam (2016). The convective heat transfer and entropy generation in either Newtonian or non-Newtonian power-law fluids with either constant or variable thermophysical properties in a parallel plate and/or a circular micro-channel were investigated by Kosar and Shojaeiam (2014, 2016) and Kiyasatfar (2018) at different boundary conditions namely no-slip and slip boundary conditions. Imal et al. (2017) numerically solved momentum and energy equations together using pseudo-spectral method based on the Chebyshed polynomials to analyze entropy generation in a non-Newtonian fluid modeled with Carreau equation with an exponential temperature dependence of viscosity.

In this study, the flow of an incompressible non-Newtonian fluid confined in a pipe with constant heat flux on the walls is analyzed to determine the temperature profiles, the entropy generation rate and the Nusselt number as functions of the power-law index, the Brinkman numbers and group parameters. This study differs from the previous studies by including viscous dissipation term in the energy equation used to compute temperature, entropy and thus the Nusselt number. It is observed that the viscous dissipation is quite effective on the temperature, the entropy and the Nusselt number. The

Nusselt number with Brinkman number and power-law index that is rather different from the previous studies (see Mahmud and Fraser, 2006) covers all types of pseudo-plastic and dilatant fluid behaviors. Furthermore, the equation with the viscous dissipation term for entropy generation number derived here is different from the previous studies since the Brinkman number in the temperature equation cause it to obtain in different shape.

THEORETICAL ANALYSIS AND MATHEMATICAL FORMULATION

Consider a steady state, incompressible non-Newtonian fluid flowing in the axial direction in a circular tube having a radius of R and a length of ℓ as shown in Fig. 1. It is assumed that the heat flux at wall is constant, the non-Newtonian fluid complied with power-law fluid model and flow is laminar and fully developed. It is considered that axisymmetric flow and thus the swirling component of velocity or θ-component of velocity (v_θ) is zero.

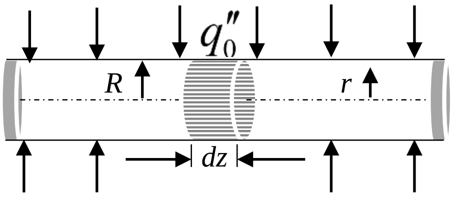

Figure 1. Schematic presentation of a circular duct.

Three-dimensional equations of the continuity and the equations of the motion in cylindrical coordinates were used to derive the one-dimensional equation for a non-Newtonian fluid flow in a pipe with the constant wall heat flux. An asymptotic analysis was used to simplify the equations of continuity and motion in dimensionless forms. Finally, the desired one-dimensional equation describing flow behavior of a non-Newtonian fluid in a tube was derived by using an approximate form of the velocity field for this geometry.

The dimensionless variables for obtaining dimensionless forms of equations of continuity and motion are defined as;

$$r = \frac{\tilde{r}}{D},\quad z = \frac{\tilde{z}}{\ell},\quad v_r = \frac{\tilde{v}_r}{v_0\left(D/\ell\right)^2},\quad v_\theta = \frac{\tilde{v}_\theta}{v_0\left(D/\ell\right)^2},$$
$$v_z = \frac{\tilde{v}_z}{v_0},\quad P = \frac{\tilde{P}}{\eta_0 v_0 \ell / D^2},\quad \eta = \frac{\tilde{\eta}}{\eta_0}$$

where ℓ is the length of the circular duct, D is the diameter of tube, v_0 is the characteristic velocity in the z-direction and v_r, v_θ, v_z are the velocities in the r, θ and z-directions. In order to preserve momentum balance in the axial direction, the pressure is scaled by the term of $\eta_0\, v_0\, \ell / D^2$ since the dominant flow occurs in this direction. The components of velocity are scaled with considering the mass conservation in the duct. The characteristic velocities in the r and θ-directions have to be proportional with v_0 because the characteristic velocity in the z-direction is larger than velocities in the r and θ-directions as expected. The dimensionless equation of continuity is obtained using the defined dimensionless variables.

$$\frac{D}{\ell}\left(\frac{1}{r}\frac{\partial}{\partial r}\left(r v_r\right) + \frac{\partial v_\theta}{\partial \theta}\right) + \frac{\partial v_z}{\partial z} = 0 \qquad (1)$$

The diameter of duct (D) is quite small with respect to the characteristic length of a circular duct (ℓ); therefore, the term of D/ℓ in Eq. (1) is much less than unity. The variations in dimensionless quantities come about over dimensionless length scales of order unity.

The dimensionless stresses can be acquired using the defined dimensionless variables as follows:

$$\tau_{rr} = \tilde{\tau}_{rr} / \left(\eta_0 v_0 D / \ell^2\right),\qquad \tau_{\theta\theta} = \tilde{\tau}_{\theta\theta} / \left(\eta_0 v_0 D / \ell^2\right)$$
$$\tau_{r\theta} = \tau_{\theta r} = \tilde{\tau}_{r\theta} / \left(\eta_0 v_0 D / \ell^2\right),\ \tau_{zz} = \tilde{\tau}_{zz} / \left(\eta_0 v_0 / D\right)$$
$$\tau_{rz} = \tau_{zr} = \tilde{\tau}_{rz} / \left(\eta_0 v_0 / D\right),$$
$$\tau_{\theta z} = \tau_{z\theta} = \frac{\tilde{\tau}_{\theta z}}{\left(\eta_0 v_0 / D\right)} = \eta\left(\delta^3 \frac{\partial v_\theta}{\partial z} + \frac{1}{r}\frac{\partial v_z}{\partial \theta}\right)$$

The steady state dimensionless momentum equations in terms of stresses in the r, θ and z-directions are, respectively, given as follows:

$$\begin{aligned} &\mathrm{Re}\,\delta^4\left[\delta\left(v_r\frac{\partial v_r}{\partial r} + \frac{v_\theta}{r}\frac{\partial v_\theta}{\partial \theta} - \frac{v_\theta}{r}\right) + v_z\frac{\partial v_r}{\partial z}\right] = \\ &-\frac{\partial P}{\partial r} + \delta^3\left[\frac{1}{r}\frac{\partial}{\partial r}\left(r\tau_{rr}\right) + \frac{1}{r}\frac{\partial \tau_{r\theta}}{\partial \theta} - \frac{\tau_{\theta\theta}}{r} + \frac{\partial \tau_{rz}}{\partial z}\right] + \delta^2 Gr \end{aligned} \qquad (2)$$

$$\begin{aligned} &\mathrm{Re}\,\delta^4\left[\delta\left(v_r\frac{\partial v_\theta}{\partial r} + \frac{v_\theta}{r}\frac{\partial v_\theta}{\partial \theta} + \frac{v_\theta v_r}{r}\right) + v_z\frac{\partial v_\theta}{\partial z}\right] = \\ &-\frac{1}{r}\frac{\partial P}{\partial \theta} + \delta^3\left[\frac{1}{r}\frac{\partial}{\partial r}\left(r\tau_{r\theta}\right) + \frac{1}{r}\frac{\partial \tau_{\theta\theta}}{\partial \theta} + \delta\frac{\partial \tau_{\theta z}}{\partial z}\right] + \delta^2 G_\theta \end{aligned} \qquad (3)$$

$$\begin{aligned} &\mathrm{Re}\,\delta\left[\delta\left(v_r\frac{\partial v_z}{\partial r} + \frac{v_\theta}{r}\frac{\partial v_z}{\partial \theta}\right) + v_z\frac{\partial v_z}{\partial z}\right] = \\ &-\frac{\partial P}{\partial z} + \left[\frac{1}{r}\frac{\partial}{\partial r}\left(r\tau_{rz}\right) + \frac{1}{r}\frac{\partial \tau_{\theta z}}{\partial \theta} + \delta^2\frac{\partial \tau_{\theta z}}{\partial z}\right] + Gz \end{aligned} \qquad (4)$$

Where;

$$\delta = \frac{D}{\ell},\ \mathrm{Re} = \frac{\rho v_0 D}{\eta_0},\ G_r = \frac{\mathrm{Re}}{Fr_r},\ G_\theta = \frac{\mathrm{Re}}{Fr_\theta},$$
$$G_z = \frac{\mathrm{Re}}{Fr_z},\ Fr_i = \frac{v_0^2}{Lg_i},\ Fr_z = \frac{v_0^2}{Dg_z}$$

Here g_i stands for the component of gravity in the i-direction, Fr_i, the Froude number in the i-direction and Re, the Reynolds number.

Since parameter of $\delta = D/\ell$ is much less than unity, the obtained dimensionless continuity and momentum equations are simplified to be following equations. Thereby, as $\delta \rightarrow 0$, Eqs. (1), (2) and (3) become respectively.

$$\frac{\partial v_z}{\partial z} = 0 \tag{5}$$

$$\frac{\partial P}{\partial r} = 0 \tag{6}$$

$$\frac{\partial P}{\partial \theta} = 0 \tag{7}$$

Eq. (5) shows velocity is independent of z-direction and Eqs. (6) and (7) point out that there are no pressure variations in r and θ-directions. In other words, the pressure has to vary in the axial direction only.

The equation of momentum in the axial direction will simplify to the following equation when letting $\delta \to 0$ for a pipe and $Re \ll 1$ for a laminar flow.

$$0 = -\frac{\partial P}{\partial z} + \left[\frac{1}{r}\frac{\partial}{\partial r}\left(r\tau_{rz} \right) + \frac{1}{r}\frac{\partial \tau_{\theta z}}{\partial \theta} \right] + Gz \tag{8}$$

The dimensionless momentum equation in the axial direction for a Newtonian or non-Newtonian fluid flow in circular is obtained in Eq. (8). Froude number in the axial direction becomes infinity because the gravitational force in this direction is zero; thereby G_z has to be equal to zero. The second term in parenthesis in Eq. (8), $\partial \tau_{\theta z} / \partial \theta$, is equal to zero since it is assumed that flow is axisymmetric. Therefore, Eq. (8) further simplifies to the following equation.

$$0 = -\frac{\partial P}{\partial z} + \frac{1}{r}\frac{\partial}{\partial r}\left(r\tau_{rz} \right) \tag{9}$$

Eq. (9) is the dimensionless form of the momentum equation for unidirectional pressure driven flow of a Newtonian or a non-Newtonian fluid in a circular duct. After obtaining its simplified form, the dimensional form of simplified equation will be taken into consideration in the solution.

The following dimensionless variables are used to non-dimensionalize the energy equation at steady state.

$$q_r = \frac{\tilde{q}_r}{q_0''}, \quad q_\theta = \frac{\tilde{q}_\theta}{q_0''\left(D/\ell \right)^2}, \quad q_z = \frac{\tilde{q}_z}{q_0''\left(D/\ell \right)},$$

$$\psi = \left(T - T_r \right) / \left(q_0'' D / k \right), \qquad z = \frac{\tilde{z}}{D\,Pe}$$

The q_r is scaled with the term of q_0'' by taking into account dominant energy transfer that takes place in radial direction. By considering energy conservation and the imposed boundary condition, the components of q were scaled as above. The characteristic heat fluxes in the θ and z-directions have to be proportional with the characteristic heat flux (q_0'') in the radial direction because the heat transfer in the r-direction is larger than those in the θ and z-directions. The previously defined dimensionless variables except $\tilde{z}$ are also used here since dimensionless z is redefined to preserve third term on left hand side of Eq. (10). The steady state dimensionless equation of energy in cylindrical coordinate (for the equation see Bird et al., 2007) is obtained as follows:

$$\begin{aligned} &Pe\left[\delta^2 v_r \frac{\partial \psi}{\partial r} + \delta^2 v_\theta \frac{\partial \psi}{\partial \theta} \right] + v_z \frac{\partial \psi}{\partial z} = \\ &-\left[\frac{1}{r}\frac{\partial}{\partial r}\left(rq_r \right) + \delta^2 \frac{1}{r}\frac{\partial q_\theta}{\partial r} + \frac{\delta}{Pe}\frac{\partial q_z}{\partial z} \right] + \left(\tau : \nabla v \right) \end{aligned} \tag{10}$$

Where Pe is the Peclet number. The dimensionless form of $\tau : \nabla v$ (for the equation of $\tau : \nabla v$ see Bird et al., 2007) is obtained with using the dimensionless stresses and velocities as follows:

$$\begin{aligned} \tilde{\tau} : \tilde{\nabla} \tilde{v} = \frac{\eta_0 v_0}{D}\frac{v_0}{D} \Bigg\{ &\delta^4 \tau_{rr}\left(\frac{\partial v_r}{\partial r} \right) + \delta^4 \tau_{r\theta}\left(\frac{1}{r}\frac{\partial v_r}{\partial \theta} - \frac{v_\theta}{r} \right) \\ &+ \frac{\delta^2}{Pe}\tau_{rz}\left(\frac{\partial v_r}{\partial z} \right) + \delta^4 \tau_{\theta r}\left(\frac{\partial v_\theta}{\partial r} \right) + \delta^4 \tau_{\theta\theta}\left(\frac{1}{r}\frac{\partial v_\theta}{\partial \theta} + \frac{v_r}{r} \right) \\ &+ \frac{\delta^2}{Pe}\tau_{\theta z}\left(\frac{\partial v_\theta}{\partial z} \right) + \tau_{zr}\left(\frac{\partial v_z}{\partial r} \right) + \tau_{z\theta}\left(\frac{1}{r}\frac{\partial v_z}{\partial \theta} \right) + \frac{\delta}{Pe}\tau_{zz}\left(\frac{\partial v_z}{\partial z} \right) \Bigg\} \end{aligned} \tag{11}$$

Where $\tau = \tilde{\tau} / (\eta_0 v_0 / D)$, $v = \tilde{v} / v_0$ and $\nabla = \tilde{\nabla} / (1/D)$. The dimensionless equation of dissipation energy can be reduced to following equation since $\delta = D/\ell$ is much less than unity. That is why, the equation of dissipation energy (Eq. (11)) becomes as $\delta \to 0$.

$$\tau : \nabla v = \tau_{zr}\left(\frac{\partial v_z}{\partial r} \right) + \tau_{z\theta}\left(\frac{1}{r}\frac{\partial v_z}{\partial \theta} \right) \tag{12}$$

As stated earlier the second term on right hand side of Eq. (12) is equal to zero for an axisymmetric flow. Thereby, Eq. (12) becomes

$$\tau : \nabla v = \tau_{zr}\left(\frac{\partial v_z}{\partial r} \right) \tag{13}$$

Eq. (13) is the equation of viscous dissipation energy for one dimensional axial flow of a Newtonian or a non-Newtonian fluid confined in a circular duct. Substituting Eq. (13) into Eq. (10) and performing simplification by taking account of the order of magnitudes of terms as $\delta \to 0$, the resulting equation becomes

$$v_z \frac{\partial \psi}{\partial z} = -\frac{1}{r}\frac{\partial}{\partial r}\left(rq_r \right) + \tau_{zr}\left(\frac{\partial v_z}{\partial r} \right) \tag{14}$$

Eq. (14) is the dimensionless equation of energy with viscous dissipation term for a one-dimensional axial flow and a one-dimensional heat transfer in radial direction. Here it is assumed that heat conduction in the axial is much less than that in radial direction by exempting a flow of liquid metal in a duct. After obtaining a one-dimensional equation of energy, the dimensional form of the simplified equation (Eq. (14)) will be considered in the solution.

ANALYTICAL SOLUTION

A power-law fluid confined in a circular duct having radius of R and length of ℓ was considered in the solution. In order to solve Eq. (9) two boundary conditions are specified as follows:

$$\tau_{rz} = \text{bounded at } r = 0 \tag{15}$$

$$v_z = 0 \text{ at } r = R \tag{16}$$

Integration of Eq. (9) once and applying the boundary condition in Eq. (15) gives following equation.

$$\tau_{rz} = \frac{1}{2}\frac{dP}{dz} r \tag{17}$$

τ_{rz} for a non-Newtonian fluid exhibiting a power-law fluid behavior is defined as:

$$\tau_{rz} = \eta_0 \left(\frac{\partial v_z}{\partial r} \right)^n \tag{18}$$

Inserting Eq. (18) into Eq. (17), and then integrating and using the boundary condition given in Eq. (16) result in the following equation.

$$v_z = v_{z\max} \left(1 - \left(\frac{r}{R} \right)^{\gamma+1} \right) \text{and } v_{z\max} = -\left[\frac{1}{2\eta_0} \left(\frac{dP}{dz} \right) \right]^{\gamma} \frac{R^{\gamma+1}}{\gamma+1} \tag{19}$$

Here γ = 1/n can be called as a modified fluid index and $v_{z\max}$ stands for maximum or centerline velocity and Eq. (19) in dimensionless form can be shown as follows:

$$v = \left(v_z / v_{z\max} \right) = \left(1 - \xi^{\gamma+1} \right) \tag{20}$$

where v and $\xi = r/R$ are dimensionless velocity in the axial direction and dimensionless distance in radial direction (dimensionless radius), respectively.

After obtaining the equation of velocity for a power-law fluid flow in a circular duct, we can deal energy equation. If Eq. (18) and the heat flux from Fourier law are inserted into Eq. (14), the energy equation in dimensional form can be expressed as follows:

$$\rho c_P v_z \frac{\partial T}{\partial z} = \frac{k}{r}\frac{\partial}{\partial r}\left(r \frac{\partial T}{\partial r} \right) + \eta_0 \left(\frac{\partial v_z}{\partial r} \right)^{n+1} \tag{21}$$

The non-dimensionless form of this equation can be obtained with introducing following dimensionless variables.

$$v = \frac{v_z}{v_{z\max}}, \quad \xi = \frac{r}{R}, \quad \zeta = \frac{z}{v_{z\max} R^2 / \alpha}, \quad \psi = \frac{T - T_r}{q_0'' R / k}$$

Introducing these dimensionless variables to Eq. (21) the dimensionless energy equation will be obtained as follows:

$$v \frac{\partial \psi}{\partial \zeta} = \frac{1}{\xi}\frac{\partial}{\partial \xi}\left(\xi \frac{\partial \psi}{\partial \xi} \right) + \left(\frac{\eta_0 c_P}{k} \right) \left(\frac{v_{z\max}^{n+1}}{\left(q_0'' R / k \right) c_P R^{n-1}} \right) \left(\frac{\partial v}{\partial \xi} \right)^{n+1} \tag{22}$$

Where $\eta_0 c_P / k$ and $v_{z\max}^{n+1} / [\left(q_0'' R / k \right) c_P R^{n-1}]$ are Prandtl number (*Pr*) and modified Eckert number (*Ec*), respectively and *Pr* × *Ec* is called as Brinkman (*Br*) number for power-law fluid. While the left hand side of Eq. (22) stands for the convection heat transfer in axial direction, the first and the second terms on the right hand side of Eq. (22) represent thermal diffusion and viscous dissipation, respectively. Since Eq. (22) is a non-homogenous partial differential equation, it may be solved with the method of separation variables and it can be assumed that the dimensionless temperature is functions of ζ and ξ in following form (Mahmud and Fraser, 2006).

$$\psi(\zeta, \xi) = f(\zeta) \times g(\xi) + f(\zeta) + g(\xi) \tag{23}$$

The first term on the right side of Eq. (23) is substantial for an initial transient and entrance effect. The second term is in Eq. (23) for considering an enhancement of axial temperature because of the accumulated wall heat flux and viscous dissipation, and the third term is important for radial temperature variations because of the wall heat flux and viscous dissipation since the viscous dissipation term is significant parameter and not disregard in the present study. It is stated earlier that the system is at steady state and entrance effects are neglected; therefore, Eq. (23) will be reduced to following form.

$$\psi(\zeta, \xi) = f(\zeta) + g(\xi) \tag{24}$$

Substituting Eq. (24) and the suitable forms of Eq. (20) into Eq. (22) gives two separate ordinary differential equations as follows:

$$\frac{\partial f}{\partial \zeta} = \frac{1}{\left(1 - \xi^{\gamma+1} \right)} \frac{1}{\xi}\frac{\partial}{\partial \xi}\left(\xi \frac{\partial g}{\partial \xi} \right) + \frac{1}{\left(1 - \xi^{\gamma+1} \right)} Br \left(-(\gamma+1) \right)^{(\gamma+1)/\gamma} \xi^{\gamma+1} \tag{25}$$

It is seen from Eq. (25) the axial temperature is directly proportional with the axial distance. Therefore, the solution of Eq. (25) will be as follows:

$$\psi(\zeta,\xi)=C_0\zeta+\left(\frac{\xi^2}{2}-\frac{\xi^{\gamma+3}}{(\gamma+3)^2}\right)C_0 -\frac{Br\left(-(\gamma+1)\right)^{(\gamma+1)/\gamma}}{(\gamma+3)^2}\xi^{\gamma+3}+C_3\ln\xi+C_4 \quad (26)$$

Here C_0 can be called as a constant of separation variable and C_3 and C_4 are integration constants.

The minus sign inside parenthesis in the term of $\left(-(\gamma+1)\right)^{(\gamma+1)/\gamma}$ comes from the derivative of velocity of a power-law fluid is not realistic since its value is positive for γ = 1 (Newtonian fluid) and it can be encountered with mathematic error even values of γ are very close to 1 such as 0.99 or 1.01. Therefore, the negative sign inside parenthesis will be dropped out hereafter since it is not possible such a dramatic change in the value of term by infinitesimal variation in γ .

In order to determine the constants C_0, C_3 and C_4, the following boundary conditions are used.

$$\psi=0 \quad \text{at } \zeta\le 0, \quad \text{for } 0\le\xi\le 1 \quad (27a)$$

$$\psi=\text{bounded} \quad \text{at } \xi=0, \quad \text{for } \zeta\ge 0 \quad (27b)$$

$$\partial\psi/\partial\xi=1 \quad \text{at } \xi=1, \quad \text{for } \zeta\ge 0 \quad (27c)$$

From Eq. (26) and boundary condition Eq. (27b) C_3 has to be equal to zero since while the left side of Eq. (26) is finite, the right side of Eq. (26) does not unless C_3 is equal to zero and from boundary condition Eq. (27c) C_0 is determined as follows:

$$C_0=\frac{2}{\gamma+1}\left[(\gamma+3)+Br(\gamma+1)^{(\gamma+1)/\gamma}\right] \quad (28)$$

Note that C_0 includes Brinkman number. C_4 can be evaluated from the mixing cup temperature defined as follows:

$$\psi_m=\frac{\int_0^{2\pi}\int_0^R v_z\psi(\zeta,\xi)rdrd\varsigma}{\int_0^{2\pi}\int_0^R v_z rdrd\varsigma}=\frac{\int_0^R v_z\psi(\zeta,\xi)rdr}{\int_0^R v_z rdr}=\frac{\int_0^1 v\psi(\zeta,\xi)\xi d\xi}{\int_0^1 v\xi d\xi} \quad (29)$$

Substituting Eq. (20) and Eq. (26) into Eq. (29) and performing the required integration yields following equation.

$$\psi_m=C_0\zeta+\frac{1}{8}\frac{(\gamma+3)}{(\gamma+5)}C_0-\frac{1}{(\gamma+3)^2(\gamma+5)}C_0 -\frac{Br}{(\gamma+3)^2(\gamma+5)}(\gamma+1)^{(\gamma+1)/\gamma}+C_4 \quad (30)$$

From the boundary condition of $\psi_m=0$ at $\zeta=0$, C_4 is determined as follows:

$$C_4=-\frac{\gamma^2+8\gamma+19}{4(\gamma+3)(\gamma+5)}-\frac{1}{4(\gamma+3)}(\gamma+1)^{(\gamma+1)/\gamma}\,Br$$

Substituting C_4 into Eq. (30) yields following equation.

$$\psi_m=\zeta\left[\frac{2(\gamma+3)}{\gamma+1}+\frac{2Br}{\gamma+1}(\gamma+1)^{(\gamma+1)/\gamma}\right] \quad (31)$$

By substituting C_3 and C_4 into Eq. (26), the equation for temperature distribution is obtained as follows:

$$\psi(\zeta,\xi)=C_0\zeta+\left(\frac{\xi^2}{4}-\frac{\xi^{\gamma+3}}{(\gamma+3)^2}\right)C_0 -\frac{Br(\gamma+1)^{(\gamma+1)/\gamma}}{4(\gamma+3)}\left(1+\frac{4\xi^{\gamma+3}}{(\gamma+3)}\right)-\frac{\gamma^2+8\gamma+19}{4(\gamma+3)(\gamma+5)} \quad (32)$$

The dimensionless wall temperature (ψ_w) can be obtained from Eq. (32) by substituting 1 for ξ and then the asymptotic difference between wall and mixing-cup temperatures is obtained as

$$\psi_w-\psi_m=\frac{\gamma^2+12\gamma+31}{4(\gamma+3)(\gamma+5)}+\frac{Br}{4(\gamma+3)}(\gamma+1)^{(\gamma+1)/\gamma} \quad (33)$$

The asymptotic Nusselt number in terms of the dimensionless wall temperature and mixing-cup temperature can be evaluated by considering the heat balance boundary condition at the internal surface of the tube wall as follows.

$$Nu_\infty=\frac{hD}{k}=\frac{2}{\psi_w-\psi_m}\left.\frac{\partial\psi}{\partial\xi}\right|_{\xi=1} =\frac{8(\gamma+3)(\gamma+5)}{\left(\gamma^2+12\gamma+31\right)+Br(\gamma+5)(\gamma+1)^{(\gamma+1)/\gamma}} \quad (34)$$

When Br is taken to be equal to zero, Eq. (34) becomes a similar equation given by Mahmud and Fraser (2006). For γ = 1 that corresponds to Newtonian fluid, the asymptotic Nusselt number becomes

$$Nu_\infty=\frac{hD}{k}=\frac{48}{11+6Br} \quad (35)$$

If Br is taken to be zero that represents the temperature of fluid is independent of viscous dissipation, the Nusselt number takes its well-known value of 4.36. As can be seen in Eq. (35) if heat transfer due to viscous dissipation is comparable with heat conduction due to temperature difference, the Nusselt number can substantially vary with Brinkman number. Eq. (34) can be used to evaluate Nusselt number for different flow situations such as slug flow, Newtonian flow and non-Newtonian flow. In other words, by using Eq. (35) the Nusselt number can be evaluated as functions of the Brinkman number and power-law index that covers all types of pseudo-plastic fluid and dilatant fluid behaviors.

ENTROPY GENERATION IN A NON-NEWTONIAN FLUID IN A CIRCULAR DUCT

Consider a power-law fluid is flowing in the *z*-direction in a horizontal circular duct. It is assumed that laminar viscous flow through the circular duct subjected to constant wall heat flux occurs for a non-Newtonian fluid with the constant physical properties (ρ, η, k, c_P). The entropy generates because of viscous dissipation of a power-law fluid flow and the constant heat flux at wall to the fluid. The volumetric rate of entropy generation for a non-Newtonian fluid flow in a circular duct can be expressed as follows (Bejan, 1979; Bird et al., 2007):

$$S_G = \frac{k}{T^2}\left[\left(\frac{\partial T}{\partial r}\right)^2 + \left(\frac{\partial T}{\partial \tilde{z}}\right)^2\right] + \frac{1}{T}\left(\tilde{\tau} : \tilde{\nabla}\tilde{v}\right) \qquad (36)$$

As can be seen from Eq. (36) the entropy generates during a Newtonian or non-Newtonian fluid flow because of the heat conduction in the spatial directions and viscous dissipation.

The previously defined dimensionless variables were used to obtain the dimensionless entropy generation rate from Eq. (36) and the dimensionless simplified form of $\tilde{\tau} : \tilde{\nabla}\tilde{v}$ (Eq. (13)) is inserted to Eq. (36) and the resulting equation is given by

$$N_S = \frac{S_G}{\left(k(q_0''R/k)^2 / R^2T_0^2\right)} = \left(\frac{\partial \psi}{\partial \xi}\right)^2 + \left(\frac{\partial \psi}{\partial \zeta}\right)^2 \frac{1}{Pe^2} + \frac{Br}{\Omega}\left(\frac{\partial v}{\partial \xi}\right)^{(\gamma+1)/\gamma} \qquad (37)$$

In order to derive the one-dimensional approximate equation for entropy generation rate of a non-Newtonian fluid flow in a circular tube, the orders of magnitude of terms were used in the dimensionless entropy generation rate equation. Here

$Pe = v_{z\max}\rho c_P R/k$, $\psi = (T - T_r)/\Delta T$, $\Delta T = q_0''R/k$, $\Omega = \Delta T / T_0$, $\Pr = c_p\eta_0/k$, $Ec = v_{z\max}^{n+1} / \left(c_p \Delta T\, R^{(n-1)}\right)$, $Br = Pr \times Ec$

The dimensionless entropy generation rate that is called as a local entropy generation number (Bejan, 1979) is given with Eq. (37) and the denominator in the first term at the right hand side of Eq. (37) is called the characteristic entropy transfer rate ($S_{G,C}$) that is equal to

$$S_{G,C} = \left[k(\Delta T)^2 / \left(R^2T_0^2\right)\right] \qquad (38)$$

It is assumed that temperature gradient in the *r*-direction is small (Bejan (1979)), that is, ψ is much less than unity in $T = T_r + \psi\Delta T$ and T can be taken equal to T_r. That is why T is taken to be equal to T_0 in Eqs. (37) and (38).
An alternative form of Eq. (37) can be given as follows:

$$N_S = N_R + N_C + N_F \qquad (39)$$

On the right hand side of Eq. (39) the first term (N_R) denotes the entropy generation by heat transfer due to the radial conduction, the second term (N_C) represents the entropy generation due to axial heat conduction and the third term (N_F) accounts for the entropy generation due to the friction among fluid particles.

The entropy generation number for a flow of a power-law fluid confined in a circular geometry is obtained by substituting the derivatives of Eq. (20) with respect to ξ and Eq. (32) with respect to ζ and ξ into Eq. (39) as follows:

$$N_S = \left\{\left(\frac{\xi}{2} - \frac{\xi^{\gamma+2}}{(\gamma+3)}\right)\left[\frac{2(\gamma+3)}{\gamma+1} + \frac{2Br(\gamma+1)^{(\gamma+1)/\gamma}}{\gamma+1}\right] - \frac{Br(\gamma+1)^{(\gamma+1)/\gamma}}{(\gamma+3)}\xi^{\gamma+2}\right\}^2 + \left[\frac{2(\gamma+3)}{\gamma+1} + \frac{2Br(\gamma+1)^{(\gamma+1)/\gamma}}{\gamma+1}\right]^2 \frac{1}{Pe^2} + \frac{Br}{\Omega}(\gamma+1)^{(\gamma+1)/\gamma}\xi^{\gamma+1} \qquad (40)$$

In literature the second term on the right hand side of Eq. (40) is dropped out for values of Peclet number larger than 4. In this study the second term on the right hand side of Eq. (40) is also dropped out for values of Peclet number larger than 4.

For a Newtonian fluid flowing in a circular tube, the equation of entropy generation number with viscous dissipation term in temperature distribution can be obtained by taking $\gamma = 1$ in Eq. (40) as follows:

$$N_S = \left\{\left(2\xi - \xi^3\right) + 2\left(\xi - \xi^3\right)Br\right\}^2 + 16(1+Br)^2/Pe^2 + 4(Br/\Omega)\xi^2 \qquad (41)$$

The obtained equation for entropy generation number for a non-Newtonian fluid flow in a circular duct is used to determine entropy generation profiles as functions of power-law index, the group parameters, the Brinkman number and the dimensionless radial distance (radius of the tube).

If Eq. (40) is compared with Eq. (39), it will be seen that each term in Eq. (39) corresponds to the term in Eq. (40) as follows:

$$N_R = \left\{\left(\frac{\xi}{2} - \frac{\xi^{\gamma+2}}{(\gamma+3)}\right)\left[\frac{2(\gamma+3)}{\gamma+1} + \frac{2Br(\gamma+1)^{(\gamma+1)/\gamma}}{\gamma+1}\right] - \frac{Br(\gamma+1)^{(\gamma+1)/\gamma}}{(\gamma+3)}\xi^{\gamma+2}\right\}^2 \qquad (42)$$

$$N_C = \left[\frac{2(\gamma+3)}{\gamma+1} + \frac{2Br(\gamma+1)^{(\gamma+1)/\gamma}}{\gamma+1} \right]^2 \frac{1}{Pe^2} \qquad (43)$$

$$N_F = \frac{Br}{\Omega}(\gamma+1)^{(\gamma+1)/\gamma} \xi^{\gamma+1} \qquad (44)$$

Eq. (42) denotes the entropy generation due to heat transfer by conduction and viscous dissipation in the radial direction and Eq. (43) represents the entropy generation due to heat transfer by conduction and viscous dissipation in the axial direction. On the other hand, Eq. (44) stands for the entropy generation due to viscous dissipation because of velocity gradient. Unlike previous studies, each terms contains viscous dissipation effect since the equation for temperature distribution has been derived by considering viscous dissipation effect that is expressed in terms of Brinkman number.

RESULTS AND DISCUSSIONS

The dimensionless entropy generation has been analyzed using the velocity and temperature distributions for a power-law fluid flow in a circular duct with constant wall heat flux. The effects of the power-law index, Brinkman number and group parameter on the temperature distribution and entropy generation number have been researched with changing one of the parameters while keeping the rest of parameters constant at certain values.

Fig. 2 illustrates variation of dimensionless velocity of a power-law fluid in a circular duct as a function of dimensionless axial distance for various values of power-law index. As can been in the figure bluntness of velocity profiles increases with decreasing power-law index. In other words, the shear layer becomes thinner with decreasing power-law index or increasing non-Newtonian behavior of a fluid. Although it is not shown in the figure, an almost linear velocity gradient can be obtained by increasing power-law index to large values (n > 10).

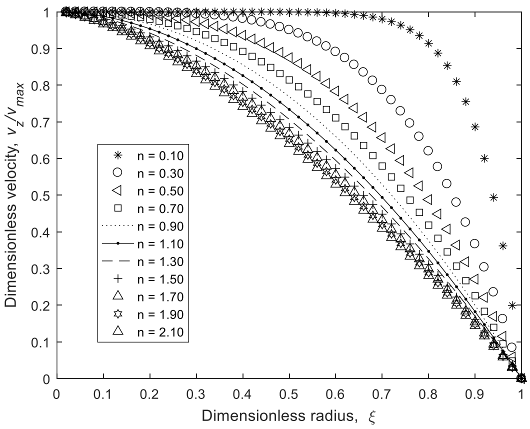

Figure 2. Dimensionless velocity profiles for various values of power-law index (*n*).

The obtained velocity expression was used in the energy equation with viscous dissipation term to obtain temperature distribution for the power-law fluid flowing in a circular duct. Dimensionless temperature (ψ) as a function of dimensionless radius at the constant axial distance of ζ = 0.1 and *Br* = 0 is presented in Fig. 3 for various values of power-law indices. As can be seen in the figure, temperature profiles increase with increasing power-law index (*n*) at any value of dimensionless radius.

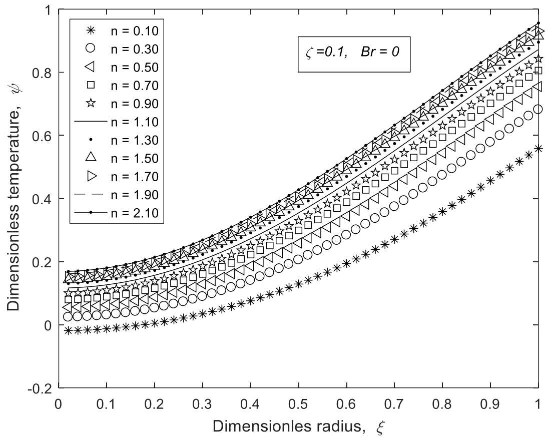

Figure 3. Dimensionless temperature as a function of ξ for various values of *n* at ζ = 0.1 and *Br* = 0.

Unlike previous studies, in the present study a viscous dissipation term is not dropped out in the energy equation (see Eq. (22)). In order to examine the effect of viscous dissipation presented here in terms of Brinkman number (*Br*), the dimensionless temperature as a function of dimensionless radius is depicted in Fig. 4 for various values of Brinkman number at the constant axial direction (ζ = 0.1) and two constant values of power-law index of *n* = 0.90 and 3.60. As can be seen in the figure the dimensionless temperature increases with increasing *Br* at any radial distance for the considered power-law indices. It is also seen that the dimensionless temperature increases with increasing power-law index at all values of Brinkman number. The comparison of Fig. 3 with Fig. 4 reveals a magnitude of dimensionless temperature with *Br* is much larger than that of dimensionless temperature without *Br*.

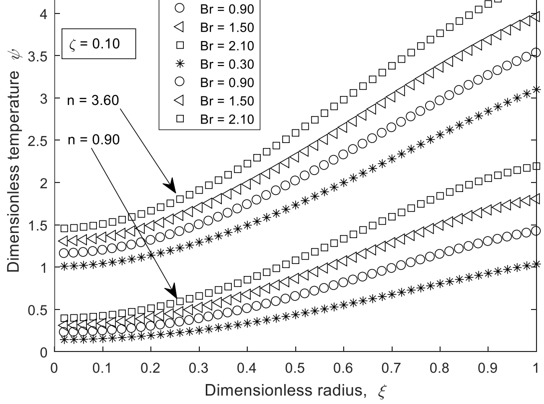

Figure 4. Dimensionless temperature as a function of ξ for various values of Br and *n* at ζ = 0.10.

Moreover, the dimensionless temperature without *Br* increases with dimensionless radius more rapidly than that containing *Br* as evidenced in Fig. 3 and Fig.4.

The dimensionless temperature (ψ) as a function of dimensionless radial distance (ξ) at constant value of power-law index (n) and Brinkman number (*Br*) is plotted in Fig. 5 for various values of the axial distance (ζ) to examine effect of the axial distance on the dimensionless temperature profiles. As seen in the figure the shape of dimensionless temperature profiles remains the same for all values of ζ at particular value of n (=0.90) but displays a shift to increasing temperature for increasing ζ since amount of thermal energy transferred to the fluid from the tube wall and the energy due to viscous dissipation increase with increasing the axial distance. In other words, due to the imposed boundary conditions, a power-law fluid inside the tube is heated by the energy generated due to viscous dissipation and thermal energy coming from the tube wall at all values of n as confirmed in Fig. 5. As can be seen in the figure the dominant heat conduction takes place in the axial direction since the dimensionless temperature changes insignificantly with the dimensionless radius at all the values of ζ. The effect of dimensionless radius on the dimensionless temperature is perceivable at low values of ζ.

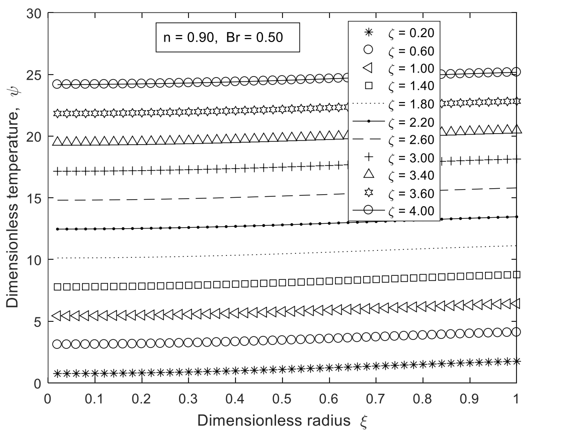

Figure 5. Variation of dimensionless temperature with an axial distance at constant n and *Br*.

The effect of the power-law index on the dimensionless temperature gradient distribution as a function of the dimensionless radius is illustrated in Fig. 6 for a constant value of Brinkman number (*Br* = 0). The dimensionless temperature gradient values in Fig. 6 are computed from Eq. (32) by taking derivative with respect to ξ and changing ξ at each specified value of the power-law index and keeping the Brinkman number zero. The figure shows that the dimensionless temperature gradient is almost linear at low values of the power-law index; for instance n = 0.1. The variation of temperature signifies the heat flux increasing linearly from zero at the center of the tube to 1 at the tube wall by conduction heat transfer between these two points and the energy generation because of viscous dissipation is not existed since *Br* is taken to be zero. An increase in the power-law index results in a non-linear temperature gradient as evidenced in Fig. 6. The temperature gradient in a power-law fluid flow in a circular duct increases with increasing power-law index at constant values of the Brinkman number (*Br* = 0) and the maximum temperature gradient takes place inside the power-law fluid near the wall about values of ξ between 0.7 – 0.9 depending on values of power-law index. The nose of dimensionless temperature gradient happens at a region between the centerline and the wall of the circular geometry. A higher entropy generation takes place at around this region since the maximum temperature gradient occurs around this region.

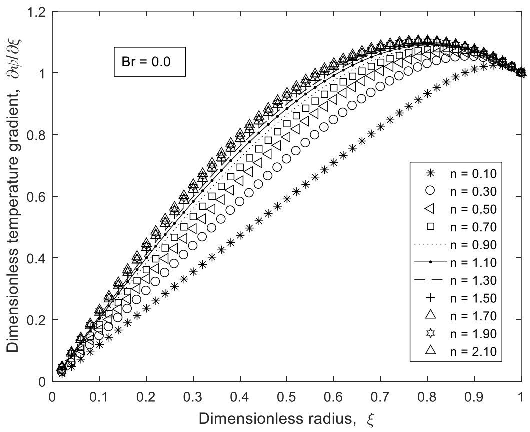

Figure 6. Dimensionless temperature gradient as a function of ξ for various values of n at $Br = 0$

Fig. 7 illustrates the effects of Brinkman number on the dimensionless temperature gradient for a specified different value of the power-law index. As can be seen in the figure, the dimensionless temperature gradient varies nonlinearly at the considered values of the Brinkman number (*Br*). The linear temperature gradient indicates that the energy due to heat conduction in the radial direction is more pronounced than the energy owing to the viscous dissipation. As seen in the figure, an increase the power-law index causes an increase in the deviation from the linearity of the temperature gradients. As seen in the figure, the temperature gradient increases with increasing power-law index.

For different values of Brinkman number, the dimensionless temperature gradients depending on the dimensionless radius are shown in Fig. 7 and Fig. 8 at the constant values of power-law index of n = 0.9 and 1.8, respectively. The energy generation on account of viscous dissipation increases with increasing the Brinkman number in Fig. 7 and Fig. 8 as expected. If one compares Fig. 6 and Fig. 7 or Fig. 8 with one another, it will be seen that the influence of the Brinkman number on the dimensionless temperature gradient is more pronounced than that of the considered values of power-law index. Furthermore, comparison of Fig. 7 and Fig. 8 with each other will reveal that the shapes of temperature profiles for different values of power-law indices (n = 0.9 and 1.8) are almost identical at the considered values of power-law indices although magnitudes of dimensionless temperature are somewhat different for the same values of Brinkman number.

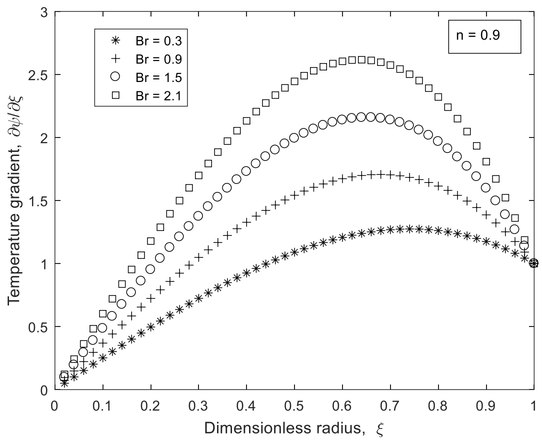

Figure 7. Temperature gradient as function of ξ for various values of Br at $n = 0.90$.

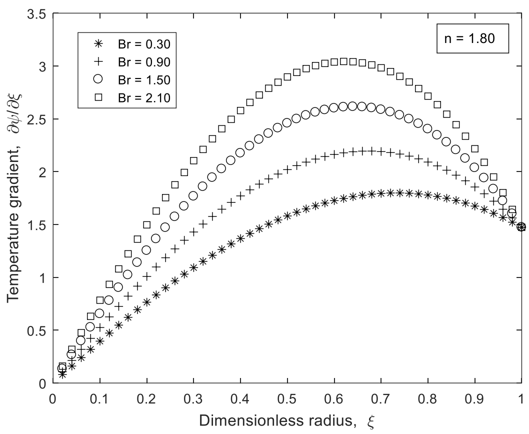

Figure 8. Temperature gradient as function of ξ for various values of Br at $n = 1.80$.

The derived dimensionless temperature expression was used in the boundary condition at the internal surface of tube wall to obtain Nusselt number that is derived functions of power-law index and Brinkman number (see Eq. (34)). The Nusselt number as a function of Brinkman number for various values of power-law index (n) is illustrated in Fig. 9. As can be seen in the figure the Nusselt number decreases exponentially with increasing Brinkman number at all values of power-law index and the effect of power-law index on the Nusselt number is getting decrease with increasing Brinkman number and eventually disappears. A decrease in the Nusselt number with increasing Brinkman number at constant value of power-law index can be attributed to variation of thermal properties of fluid such as an increase in thermal conductivity and a decrease in density of the fluid with increasing temperature due to viscous dissipation. Fig. 10 shows the variation of Nusselt number with power-law index at constant value of Brinkman number ($Br = 0$). As can be seen in the figure the Nusselt number decreases exponentially with increasing power-law index and it takes its well-known value of 4.36 at $n = 1$ (Newtonian fluid). A decrease in Nusselt number with increasing power-law index can be attributed to an increase in the film thickness of fluid on the tube surface that may cause heat transfer coefficient to decrease in the internal surface of a circular tube wall since the shear layer becomes thicker with increasing power-law index (see Fig. 2).

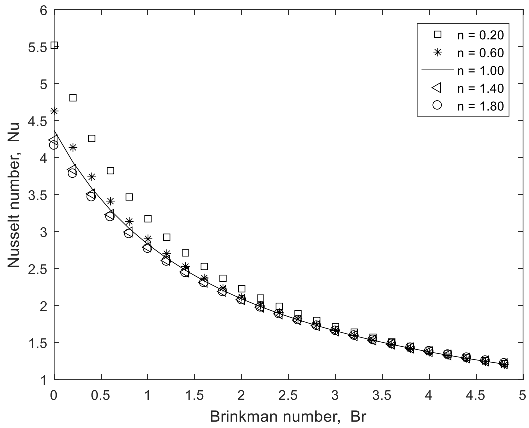

Figure 9. Nusselt number as function of Brinkman number for various values of n.

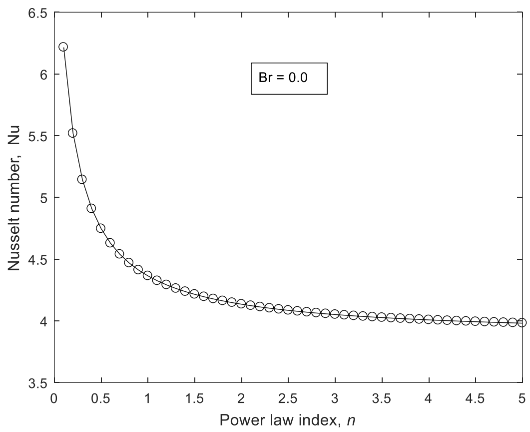

Figure 10. Nusselt number as a function of power-law index (n) at $Br = 0$.

The entropy generation in the non-Newtonian fluid flow in a circular duct was analyzed using the obtained equations for velocity and temperature gradients. In this context, to determine the effect of the power-law index on the entropy generation, the dimensionless entropy generation number as a function of the dimensionless radius is depicted in Fig. 11 for constant values of the Brinkman number ($Br = 0$) in the equation of temperature gradient and the group parameter ($Br/\ \Omega = 0$) in the equation of entropy generation. Eq. (40) was used to compute the entropy generation values by changing ξ at each specified value of the power-law index while keeping the Brinkman number and the group parameter being zero. Fig. 11 illustrates that the dimensionless entropy generation rate increases insignificantly with increasing the power-law index at all values of the dimensionless radius. The tip of entropy generation rate locates between the centerline and the wall of tube, which occurs at the maximum velocity gradient (see velocity profiles). Furthermore, there is no entropy generation at centerline for each specified value of the power-law index. This figure agrees with Fig. 6 in which the nose of temperature gradient at each specified value of the power-law index has developed in a region between the centerline and the tube wall. The minimum temperature gradient will produce the minimum entropy generation. It is also seen in the figure the entropy generation near the walls is larger than that in any other locations in the circular duct. Therefore, the larger velocity and temperature gradients near the walls cause larger entropy generation in the same region. Furthermore, when *Br* and *Br/Ω* are, respectively, taken to be zero in the equations of temperature gradient and entropy generation rate, the entropy generation at each considered value of the power-law index displays a similar trend.

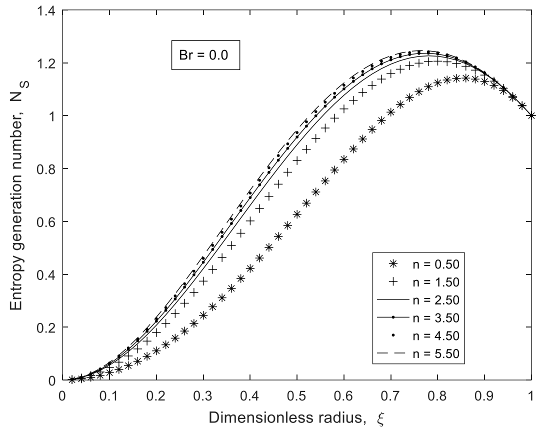

Figure 11. Entropy generation number as function of ξ for various values of *n* at *Br* = 0.

Fig. 12 depicts that the entropy generation number versus dimensionless radial distance at different values of *Br* for constant values of power-law index (*n* = 0.9) and group parameter (*Br/Ω* = 0). The effect of Brinkman number on the entropy generation rate is much more pronounced than on temperature as evidenced in Fig. 12 although the group parameter in the equation of entropy generation rate is taken to be zero. As can be seen in the figure an increase in Brinkman number increases the entropy generation at a constant value of power-law index. As mentioned previously there is no entropy generation at the centerline of the tube at all the values of Brinkman numbers and the entropy generation rate reaches the maximum value at the values of dimensionless radius between 0.6 and 0.75 depending on values of Brinkman number and is equal to 1.0 at the wall of circular duct due to the imposed boundary condition on it.

In order to evaluate the effect of the group parameter (*Br/Ω*) on the entropy generation for two different values of the power-law index, the entropy generation number versus the dimensionless radius are depicted in Fig. 13 and Fig. 14 at different values of *Br/Ω*. The entropy values in Fig. 13 and 14 were calculated from Eq. (40) by varying the ξ while keeping the power-law index constant at values of 0.9 and 2.7, respectively. The figure displays that an increase in the group parameter (*Br/Ω*) causes an increase in the entropy generation number at constant values of power-law index. The entropy generation number at a value of *Br/Ω* = 0.45 is much less than that at the high value of *Br/Ω* = 2.10. There is no entropy generation rate at the centerline of the circular duct for all the values of *Br/Ω* and the entropy generation rate increases substantially with increasing the dimensionless radius (ξ) at all values of group parameter. Therefore, the effect of dimensionless radius on the entropy generation rate is pronounced at the considered values of group parameter as confirmed in Fig. 13 and Fig. 14. Owing to high temperature and velocity gradients near the walls, it can be said that circular duct walls behaves as an irreversibility producer at high values of group parameter. If one compares Fig. 13 and Fig. 14 with one another, it will be seen that the effect of group parameter on the entropy generation is more pronounced at the high value of power-law index (*n* = 2.7) than at the low value of power-law index (*n* = 0.9). As seen in those figures entropy generation rates are not ended at value of 1.0 since viscous dissipation effect becomes more effective with increasing *Br* and *Br/Ω* and the end points of profiles increase with increasing group parameter.

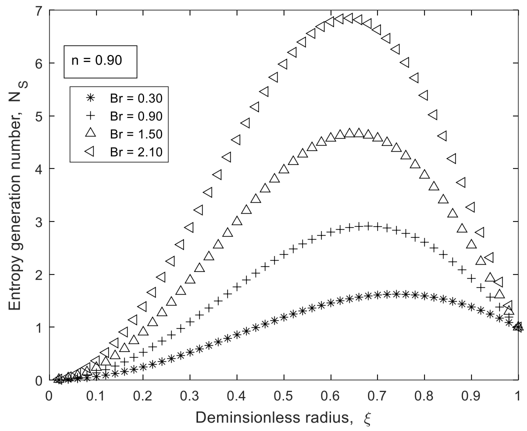

Figure 12. Entropy generation number as function of ξ for various values of Br at *n* = 0.90.

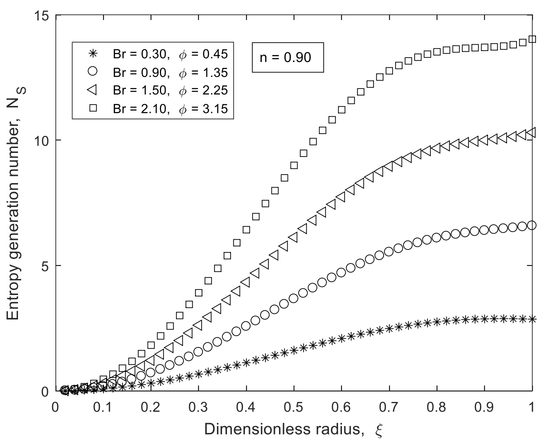

Fig. 13. Entropy generation number as function of ξ for various values of *Br* and ϕ at *n* = 0.90.

The dimensionless entropy generation number (*Ns*) as a function of dimensionless radius (ξ) is depicted in Fig. 15

for various values of Brinkman number and group parameter at constant Peclet number. The local heat transfer irreversibility remains almost constant with increasing dimensionless radial distance (ξ), which means the term coming from the axial conduction (Eq. (43)) is dominant over the term coming from the radial conduction (Eq. (42)) and the viscous dissipation as in temperature distribution obtained by considering axial conduction (see Fig. 5). As seen from Eq. (43) and Eq. (42) both terms, the one coming from the axial conduction and the other coming from the radial conduction include the Brinkman numbers (viscous dissipation). As seen in Fig. 15 the entropy generation number increases with increasing values of Brinkman number and group parameter at constant Peclet number and it is also seen that the entropy generation number decreases with increasing Peclet number at all values of *Br* and Br/Ω since the term coming from the axial heat conduction decreases with the square of the Peclet number (see Eq. (43)).

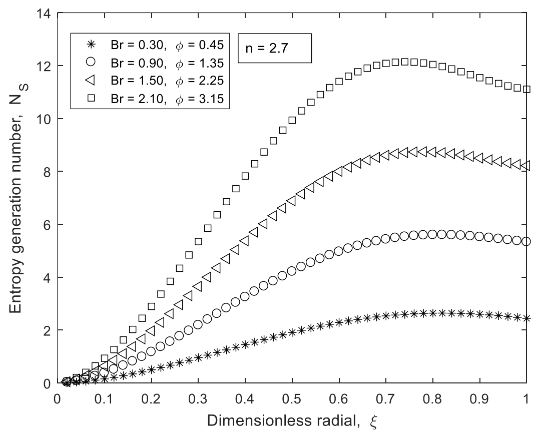

Figure 14. Entropy generation number as function of ξ for various values of *Br* and ϕ at $n = 2.7$.

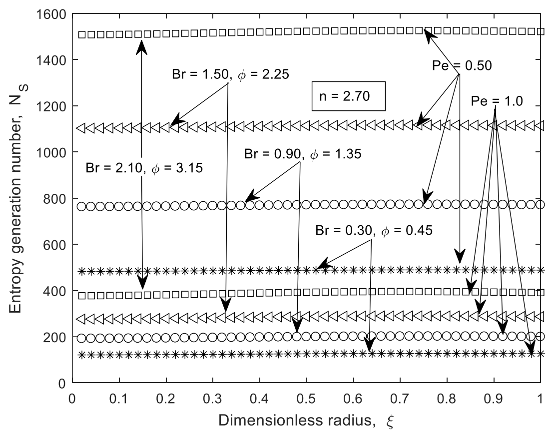

Figure 15. Entropy generation number as function of ξ for various values of *Br* and ϕ at $Pe = 0.5$-1.0 and $n = 2.70$.

In order to examine effects of *Br* and Br/Ω on the irreversibility ratio as a function of the dimensionless radius (ξ), Fig. 16 is plotted for various values of *Br* and Br/Ω at constant value of power-law index of 0.90 and Pe^{-2}. As can be seen in the figure the irreversibility ratio increases with increasing *Br* and Br/Ω at all location in the fluid. However the effects of *Br* and Br/Ω on the irreversibility ratio is negligible at the low values of dimensionless radius (0-0.6) for all values of *Br* and Br/Ω. The irreversibility ratio begins to increase exponentially with increasing the dimensionless axial distance at $\xi = 0.6$ for all considered values of *Br* and Br/Ω except the values of $Br = 0.10$ and $Br/\Omega = \phi = 0.15$. As mentioned previously a high velocity gradient near the tube wall contribute a major portion of entropy generation due to the friction of fluid particles. It can be seen in Fig. 2 the velocity gradient is higher in magnitude as *n* takes lower values although Fig. 16 is depicted for a constant value of power-law index of 0.9.

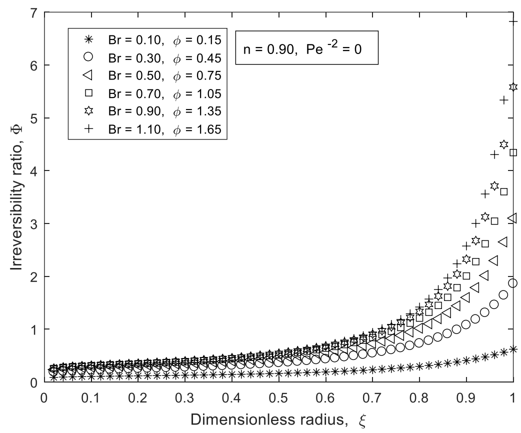

Figure 16. Irreversibility ratio as a function of ξ for various values of *Br* and ϕ at $Pe^{-2} = 0$ and $n = 0.90$.

It is known that *Br* is much less than unity for many engineering processes (Bejan, 1979). The ratio of entropy generation due to the friction of fluid particles (N_F) to heat transfer (N_R+N_C) is known to be irreversibility distribution ratio that is equal to the ratio of Brinkman number to the dimensionless temperature difference (Br/Ω). Here ϕ stands for the irreversibility distribution ratio. That is why values of ϕ are less than unity mean irreversibility due to heat transfer is higher than that owing to fluid friction. Otherwise, the irreversibility because of fluid friction dominates over that due to heat transfer ($\phi > 1$). The irreversibilities due to heat transfer and fluid friction are comparable and make the same contribution to entropy generation when $\phi = 1$. Paoletti et al. (1989) defined an alternative irreversibility distribution parameter, called Bejan number, given by

$$\phi = \frac{N_F}{N_R + N_C} \quad \text{and} \quad Be = \frac{N_R + N_C}{N_R + N_C + N_F} = \frac{1}{1+\phi} \qquad (45)$$

Eq. (45) points out that Bejan number is a ratio of entropy generation due to heat transfer to the total entropy generation. As can be seen from Eq. (45) the interpretation just made above can be made using Bejan number. Its values have to be between 0 and 1. The irreversibility on account of heat transfer dominates over the irreversibility due to fluid friction when $Be = 1$, which means the value of ϕ is less than unity namely $\phi = 0$. If the irreversibility owing to fluid friction is much higher than that because of the heat transfer, *Be* can be equal to zero, which corresponds to the limit of $\phi \rightarrow \infty$. if *Be* = 1/2, that the irreversibilities owing to heat transfer and fluid friction have the same contribution to entropy generations, which is identical to the case of $\phi = 1$.

Fig. 17 is depicted for variation of the global entropy generation number per unit length as a function of power-law index for the selected values of Brinkman and group parameter at constant Peclet number (= 1.0).

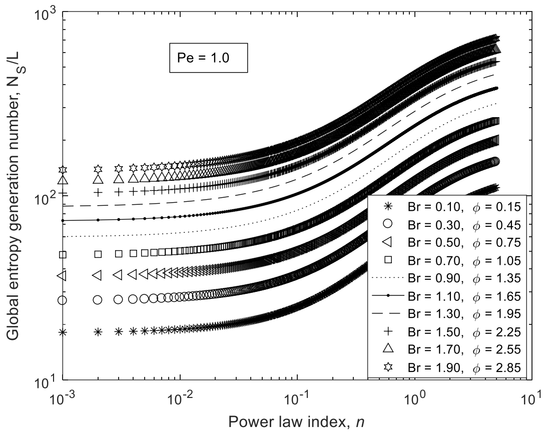

Figure 17. Global entropy generation number per unit length as a function of n for various values of *Br* and ϕ at *Pe* = 1.0.

The magnitude of *Ns/L* is larger for larger values of Brinkman number and group parameter at a particular value of *n*. As seen in the figure, the global entropy generation number per unit length increases with increasing values of the Brinkman number and group parameter at all values of power-law index. The global entropy generation remains almost constant up to a value of power-law index reaches to 0.1 and begins to increase at this value as evidenced in Fig. 17. In other words, the power-law index is not effective on global entropy generation for low values of power-law index ($n < 0.10$). As can be seen in the figure, the power-law index has a substantial effect on the global entropy generation in pseudo plastic and dilatant fluids when the viscous dissipation is taken into consideration in the energy equation. The minimum for entropy generation takes place at a minimum value of power-law index for all values of *Br* and Br/Ω. The profiles of global entropy generation numbers seem to illustrate asymptotic behavior for dilatant fluids when $n > 3$.

CONCLUSIONS

The velocity, the temperature, the Nusselt number and the entropy distributions for the flow of a power-law fluid in a circular duct have been determined as functions of the influential parameters such as the power-law index, the Brinkman number, the group parameter and the irreversibility ratio. The one-dimensional equations for the velocity, the temperature and entropy generation rate for an incompressible non-Newtonian fluid flowing in a circular duct have been obtained from simplification of momentum, the energy and entropy equations by asymptotic techniques. Those equations for the velocity, the temperature and entropy generation rate have been analytically solved and used to determine distributions of those variables. It have been observed that the velocity profiles of a non-Newtonian fluid flowing in a circular geometry become blunter with decreasing the power-law index and thus, the heat generation owing to the viscous dissipation shifts to near the tube wall. It has been also observed that the changes of the temperature gradient as a function of the dimensionless radius is linear between the centerline and the tube wall at the low values of power-law index ($n = 0.1$). It is concluded that the deviations from the linearity of temperature gradient increase with increasing the power-law index since the temperature gradient in the non-Newtonian fluid becomes higher near the wall of circular duct. The similar trend with different magnitudes in the temperature gradient has been observed for variations of the Brinkman number. The temperature gradient increased substantially in the fluid with increasing the Brinkman number. It has been observed that the viscous dissipation term is significant parameter on Nusselt number since it varies substantially with the variations of the Brinkman number at a constant value of power-law index. Brinkman number dramatically affects the Nusselt number that has exponentially decreased with increasing the Brinkman number at all values of power-law index. In addition, the Nusselt number has exponentially decreased with increasing the power-law index at the certain values of Brinkman number and it took well-known value of 4.36 at $n = 1$ (Newtonian fluid). The effect of power-law index on the Nusselt number has gotten decrease and eventually disappeared with increasing values of Brinkman number. The entropy generation distribution is dependent on the velocity and the temperature gradients. While the entropy generation rate increases insignificantly with increasing the power-law index, it increases substantially with increasing the Brinkman number and group parameter at the certain values of power-law index.

REFERENCES

Bejan, A., 1979, A study of entropy generation in fundamental convective heat transfer, *J Heat Transf,* 101, 718-725.

Bejan, A., 1996, Entropy generation minimization. New York, CRC Press.

Bejan, A., 1982, Second law analysis in heat transfer and thermal design, *Adv. Heat Transfer*, 15, 1-58.

Bird, R. B., Stewart, W. E. & Lightfoot, E. N., 2007, Transport phenomena. Revised 2nd Edition, Wiley, New York.

Imal, M; Ozalp, C; Yaniktepe, B; Mehdi-Rashidi, M; & Hurdogan, E., 2017, Entropy generation for a non-Newtonian shear thinning fluid with viscous heating effects. *Trans. Canadian Soc. Mech. Eng.*, 41, 593-607.

Kamisli, F., 2009, Analysis of laminar flow and forced convection heat transfer in a porous medium. *Transport in Porous Media*, (80) 345-371.

Kamisli, F., 2008, Second law analysis of a disturbed flow in a thin slit with wall suction and injection, *Int. J. Heat Mass transf.*, 51 3985-4001.

Kamisli, F. & Oztop, H. F., 2008, Second law analysis of 2D laminar flow of two-immiscible, incompressible viscous fluids in a channel. *Heat and Mass transf.*, 44, 751-761.

Kiyasatfar, M., 2018, Convective heat transfer and entropy generation analysis of non-Newtonian power-law fluid flows in parallel-plate and circular microchannels under slip boundary conditions, *Int. J. Thermal Sci.*, 128, 15–27.

Mahmud, S. & Fraser, R. A., 2006, Second law analysis of forced convection in a circular duct for non-Newtonian fluids. *Energy*, (31) 2226-2244.

Mukherjee, S., Gupta, A.K. & Chhabra, R.P., 2017, Laminar forced convection in power-law and Bingham plastic fluids in ducts of semi-circular and other cross-sections, *Int. Journal Heat and Mass Transfer*, 104, 112-141.

Nag, P. I. K. & Kumar, N., 1989, Second law optimization of convective heat transfer through a duct with constant heat flux. *Int. J. Energy Res.* (13) 537-543.

Narusawa, U., 2001, The second law analysis of mixed convection in rectangular ducts, *Heat Mass Transf.*, 37, 197-203.

Paoletti, S., Rispoli, F. & Sciubba, E., 1989, Calculation energetic loses in compact heat exchanger passages, *ASME AES*, 10, 21–29.

Sahin, A. Z., 1998, Second law analysis of laminar viscous flow through a duct subjected to constant wall temperature, *J. Heat Transf.*, 120, 76-83.

Sahin, A. Z., 1998, A second law comparison for optimum shape of duct subjected to constant wall temperature and laminar flow, *Heat Mass Transf.*, 33, 425-430.

Sahin, A. Z., 1999, Effect of variable viscosity on the entropy generation and pumping power in a laminar fluid flow through a duct subjected to constant heat flux, *Heat Mass Transf.*, 35, 499-506.

Sahin, A. Z., 2014, A Simple method of determining entropy generation rate in viscous fluid flow through ducts, *Arab J. Sci. Eng.*, 39, 1241–1249.

Saouli, S. & Saouli. S.A., 2009, Second law analysis of laminar non-Newtonian gravity-driven liquid film along an inclined heated plate with viscous dissipation effect, *Brazilian J. Chem. Eng.*, 26, 407-414.

Sarabandi, A.H. & Moghadam, A.J., 2017, Thermal analysis of power-law fluid flow in a circular microchannel, *J. Heat Transfer*, 139, 1-14 (032401).

Shojaeian, M. & Kosar, A., 2014, Convective heat transfer and entropy generation analysis on Newtonian and non-Newtonian fluid flows between parallel-plates under slip boundary conditions, *Int. J. Heat and Mass Transfer*, 70, 664–673.

Shojaeian, M. & Kosar, A., 2016, Convective heat transfer of non-Newtonian power-law slip flows and plug flows with variable thermophysical properties in parallel-plate and circular microchannels, *Int. J. Thermal Sci.*, 100, 155-168.

Dr. Fethi Kamisli graduated from Istanbul Technical University with B.Sc. degree in Department of Chemical Engineering. Following years to his graduation from Istanbul Technical University, he got the position in the Department of Chemical Engineering at Firat University as a teaching and research assistant. During this position Mr. Kamisli earned the scholarship from the Turkish government for studying Ph.D degree in the United State of America. Mr. Kamisli graduated from the State University of New York at Buffalo with Ph.D degree in 1997. After getting Ph.D. degree from SUNY, Dr. Kamisli came back to Firat University and from that date he has been teaching some courses at undergraduate and graduate level in the Department of Chemical Engineering at Firat University. He was invited to the International Conference on Models and Methods in Fluids Mechanics in Abbottabat-Paskistan as an invited speaker for two lectures of one hour each and was also invited to International Conference on Frontier of Mathematics & Applications in The University of Burdwan Golapbag, Bardhaman - 713 104 West Bengal, INDIA. Dr. Kamisli has also been working as a reviewer in International Journal for Numerical Methods in FLUIDS, International Journal of Heat & Mass Transfer, Journal of Transactions of the Canadian Society for Mechanical Engineering, Applied Thermal Engineering, Chemical Engineering and Processing, Journal of Materials Processing Technology and Journal of Pure and Applied Chemistry. He had participated in the course of the Organization for the Prohibition of Chemical Weapons (Associate Programme 2006, OPCW) and recently participated in International Summer School on Fuel Cells Fundamentals in July 17-20th, 2007, Sibiu, Romania. Dr. Kamisli is coordinator of ERASMUS in the department of chemical engineering. In this context he has visited some universities in European countries and given lectures on different subjects in chemical engineering. Dr. Kamisli has some industrial experiences such as practicing internship in oil refinery for two months and internship in the sugar beet processing plant for one month. He has also worked with local factories as a consultant. He has published 19 research papers in international scientific journals in the science citation index and 15 research papers in national scientific journals. Dr. Kamisli has attended many national and international conferences related to the fields of chemical engineering and he has published the text book of Heat Transfer and took part in translation of the book of Chemical Engineering Design.